ResearchGate

See discussions, stats, and author profiles for this publication at: https://www.researchgate.net/publication/330266248

UAV Formation Flight Cooperative Tracking Controller Design

Conference Paper · November 2018

DOI: 10.1109/ICARCV.2018.8581093

CITATIONS
7

READS
80

5 authors, including:

Jialong Zhang
Northwestern Polytechnical University
15 PUBLICATIONS **62** CITATIONS
SEE PROFILE

Maolong Lv
Delft University of Technology
5 PUBLICATIONS **23** CITATIONS
SEE PROFILE

Xiangjie Kong
Zhejiang University of Technology
138 PUBLICATIONS **2,231** CITATIONS
SEE PROFILE

Some of the authors of this publication are also working on these related projects:

Project Data-Driven Academic Collaboration Behaviors Analytics View project

Project UAV formation tracking control View project

All content following this page was uploaded by Jialong Zhang on 19 May 2019.

The user has requested enhancement of the downloaded file.

2018 15th International Conference on
Control, Automation, Robotics and Vision (ICARCV)
Singapore, November 18-21, 2018

UAV Formation Flight Cooperative Tracking Controller Design

JIALONG ZHANG*, JIANGUO YAN, MAOLONG LV, XIANGJIE KONG, *Senior Member, IEEE*
AND PU ZHANG

***Abstract*— Aiming at the collision between the unmanned aerial vehicles (UAVs) in tracking motion target due to the inconsistency information, we design the unmanned aerial vehicle (UAV) formation cooperative tracking controller and analyze the flight-stability of the designed controller in the case of only knowing the UAV local information. Recently, a Lyapunov guidance vector field approach is proposed to achieve the desired circular trajectory in the paper. The path planning of a single UAV and the Multi-UAVs cooperative formation tracking motion target are simultaneously studied. In the ideal case, a guidance vector field method is proposed for the heading convergence, which has the advantage of analyzing and solving the collision problem between the unmanned aerial vehicles (UAVs). Further, a variable airspeed controller is used to maintain the UAV cooperative formation flight in a circular orbit, and an adaptive estimate is introduced to ensure the flight-stability of a circular orbit in the case of unknown wind and moving targets. In the process of the UAV formation tracking motion targets, we use a variable airspeed controller to achieve the desired angular spacing. In this paper, the designed controller laws are decentralized based on the local information. Meanwhile, the simulation shows that the designed controller has a good the flight-stability in the process of tracking motion target.**

I. INTRODUCTION

Recently, the multi-agent formation control has made great achievements. It has also gradually been applied to various fields and completed various tasks in a cooperative way. Moreover, the issue of Multi-UAVs cooperative formation control has been studied [1-10]. An agent can measure the relative distance from the adjacent agent and control displacement to achieve the desired formation. However, the reference frame of local agent is consistent with the global coordinate system by using this control method. For the single integrator, double integrator and multiple integrator systems, the flight-stability of the UAV formation is introduced in local reference cooperative system, while the local reference cooperative system is inconsistent with the literature [6-8]. Although the agents can measure the relative position of the adjacent agents, they do not directly control the relative positions between them because they do not have the same sense of orientation. There are also a large number of studies on the UAV cooperative formation control [11-12], concluding path planning, optimal perceptual geometry, distributed control laws design, and information architecture. Obviously, these different aspects of the cooperative control problems require to be unified into the framework. However, this is a very complicated task. They are not only many important aspects, but also these aspects are interrelated. This paper mainly studies two key aspects, including the distributed control laws design and extended information architecture. Moreover, we illustrate their convergence via the cooperative tracking problem.

An important use of UAV is to detect and track the motion targets. The UAV formation could be used to engage and assess unknown or adversarial targets to provide reconnaissance or detect potential threats around the surrounding environment, which can play a good guarding role in many aspects. In the cooperative tracking of the UAV formation, the Multi-UAVs are only to use local information to flight in a circular orbit around a moving obstacle with predetermined angular spacing. In the case of the known a given target's attitude and position information, the UAV can distribute around the target with the optimal geometry at equal angles [13]. In recent years, Frew and Lawrence proposed a Lyapunov guidance vector field method to maintain a prescribed tracking radius [14]. Their study neglected an important timescale separation issue, including heading and radius convergence. Further, they analyzed that any two UAVs can achieve a prescribed angular spacing with vary airspeeds while moving a circular orbit around the motion target did not provide complete convergence proof. For the tracking problem, Kingston and Beard also used a Lyapunov guidance vector field approach to the tracking problem and only used the heading to obtain the desired circular orbit and spatial position [15]. However, they neglected the timescale separation issue by using a dynamic sliding mode controller to ensure the heading convergence in finite time. They also used the symmetrical information structure of the UAV formation to expand the number of UAVs and given some flight-stability results.

Based on the deficiencies in the studies of the above scholars, we further study the Lyapunov guidance vector field approach to fly in the desired circular orbit. We also propose a heading convergence method by addressing the time-scale separation problem, which takes advantage of the guidance

*Research supported by the National Natural Science Foundation of China under Grant 61873207.

JIALONG ZHANG* is with the School of Automation, Northwestern Polytechnical University, xi'an, 710129, China. His phone: 18392005957; e-mail: zjl0117@mail.nwpu.edu.cn.

JIANGUO YAN is with the School of Automation, Northwestern Polytechnical University, xi'an, 710129, China. His e-mail: yjg0311@nwpu.edu.cn.

MAOLONG LV is with Delft Center for Systems and Control, Delft University of Technology, Mekelweg 2, Delft 2628 CD, The Netherlands. His e-mail: M.Lyu@tudelft.nl.

XIANGJIE KONG is with the Key Laboratory for Ubiquitous Network and Service Software of Liaoning Province, School of Software, Dalian University of Technology, Dalian, 116620, China. His email: xjkong@ieee.org.

PU ZHANG is with the School of Automation, Northwestern Polytechnical University, xi'an, 710129, China. Her e-mail: 18789464152@163.com.

filed. To keep the UAV formation flight in a circular orbit, we use a variable airspeed controller to control the UAV formation. We can achieve the purpose of the UAV formation cooperative tracking problem with a rigid graph theory, while we use two types of information architectures, including symmetrical and asymmetric structures, and use them to design the decentralized control law. These information architectures can be extended Multi-UAVs, in other words, as the number of UAVs increase linearly, the number of information communication links between UAVs increase. Moreover, the designed control law is distributed using only local information.

In this paper, we design a cooperative controller for the UAV formation tracking motion target and model the information architecture, and then analyze the flight-stability of the controller. In Section II, the UAV dynamics model and the Lyapunov guidance field approach are proposed. In the case of the no-wind and stationary target, the guidance field can provide an analytical solution in the process of the UAV close formation and be applied to the path planning for a single UAV. In section III, we propose a variable airspeed control law and use two different information architectures to achieve desired the angular spacing. In section IV, we present the global convergence of any two UAVs and verity the validity of the designed controller by using the numerical simulation, and provide a theoretical reference for the UAV formation tracking motion target. Finally, the concluding remarks are stated in Section V.

II. THE MODEL OF UAV

The section establishes the dynamic model of a single UAV in the desired circle orbit, and presents a Lyapunov guidance vector field method. We firstly study the dynamic characteristics of a single UAV with the no-wind, stationary target case and then generalize these results to unknown wind and moving targets.

The dynamic model of a single fixed-wing UAV with kinematic constraints is as follows:

$$\begin{cases} \dot{x} = \mu_1 \cos\psi \\ \dot{y} = \mu_2 \sin\psi \\ \dot{\psi} = \mu_2 \end{cases} \tag{1}$$

where $[x, y]^T \in R^2$ is the position of the UAV's inertial coordinates, ψ is heading angle, μ_1 is the command of airspeed, μ_2 is the command of heading. This is a simplification of the real UAV. It is known that the UAV can maintain stability in the vertical direction. However, the model analysis of UAV is more complicated in the horizontal plane, and the input dynamics with the second order control are easily ignored. Moreover, a single UAV was studied both in the horizontal plane and in the vertical direction, which is also a comprehensive describing UAV motion in the literature [14,16-17]. It has essential significance for applying dynamic constraints to the model in the actual project. Suppose that there are constraints on the maximum and minimum airspeed based on the inequation (2):

$$0 < \upsilon_{\min} \le \mu_1 \le \upsilon_{\max} \tag{2}$$

then the heading angular rate constraint is based on inequation (3):

$$|\mu_2| \le \omega_{\max} \tag{3}$$

The maximum heading angular rate constraint is equivalent to a minimum turning radius constraint, where $r_{\min} = 4\mu_1/\omega_{\max}$, the heading angular and airspeed commands are generated from a Lyapunov vector field that guides the UAV in a circular orbit around the target, while the target is stationary. Consider the Lyapunov function, as shown in the equation (4):

$$V(r) = \frac{1}{2}\left(r^2 + r_d^2\right)^2 \tag{4}$$

where $r = \sqrt{x^2 + y^2}$ is relative distance between UAV and target, r_d is the desired tracking circular orbit radius. To achieve the motion of the UAV in a circular orbit, we choose desired inertia velocity based on the vector field. Its vector field is as follows:

$$f(x,y) = \begin{bmatrix} \dot{x} \\ \dot{y} \end{bmatrix} = -\frac{\mu_o}{r\left(r^2 + r_d^2\right)} \begin{bmatrix} x\left(r^2 - r_d^2\right) + y\left(2rr_d\right) \\ y\left(r^2 - r_d^2\right) - x\left(2rr_d\right) \end{bmatrix} \tag{5}$$

where μ_0 is the relative airspeed of UAV. The guidance vector field is expressed in polar coordinates, as shown in equation (6):

$$g(r,\theta) = \begin{bmatrix} \dot{r} \\ r\dot{\theta} \end{bmatrix} = \frac{\mu_0}{r^2 + r_d^2} \begin{bmatrix} -\left(r^2 - r_d^2\right) \\ 2rr_d \end{bmatrix} \tag{6}$$

Qualitative analysis that when $r > r_d$, r decreases toward the desired circular orbit radius; when $r < r_d$, r is increases away from the desired circular orbit radius; when $r = r_d$, r is the desired circular orbit radius with a constant angular speed of $\dot{\theta} = \mu_0 / r_d$, this is an ideal case. We calculate these trajectories using the derivative of Eq. (4), as shown in the following equation:

$$\dot{V} = -\frac{4\mu_0 r\left(r^2 - r_d^2\right)^2}{r^2 + r_d^2} \le 0 \tag{7}$$

According to LaSalle's principle of invariance, the trajectory of the UAV converges asymptotically to the desired orbit radius [14]. In fact, the vector field is an approximate analytical method. Observe that the kinematics equation 6 is independent of θ, and the Eq. (8) can be obtained, as shown in the following formula:

$$\frac{dr}{d\theta} = \frac{r^2 - r_d^2}{2rr_d} \tag{8}$$

And we can obtain its solution:

$$\begin{cases} r(\theta) = \dfrac{1 + k_r e^{-\theta}}{1 + k_r e^{-\theta}} r_d \\ k_r = \dfrac{r_0 - r_d}{r_0 + r_d} \end{cases} \tag{9}$$

where $r_0 = r(0)$ is initial separation distance between the UAV and the target. Substituting this solution into the Eq. (6), we can obtain a function of time, as shown in the following formula:

$$\theta - \theta_0 = \frac{\mu_0}{r_d} t + 2k_r \left[\frac{e^{-\theta}}{1 - k_r e^{-\theta}} - \frac{e^{-\theta_0}}{1 - k_r e^{-\theta_0}} \right] \tag{10}$$

where θ_0 is initial heading angular in the polar coordinate.

The solution of Eqs. (9) and (10) contain complete analytical solutions, hence, the trajectory of UAV is known. The heading angular along the vector field, denoted by ψ_d, which is obtained by Eq. (11):

$$\psi_d = \arctan(\frac{\dot{y}}{\dot{x}}) = \arctan(\frac{y\left(r^2 - r_d^2\right) - x\left(2rr_d\right)}{x\left(r^2 - r_d^2\right) + y\left(2rr_d\right)}) \tag{11}$$

The derivative of Eq. (11) is given by

$$\dot{\psi}_d = \frac{4\mu_0 r_d^3}{\left(r^2 + r_d^2\right)^2} \tag{12}$$

To satisfy the constraints of heading angular rate, we can obtain $|\dot{\psi}_d| < \omega_{\max}$, namely, which is equivalent to $4\mu_0 / r_d < \omega_{\max}$ by using μ_0 and r_d.

According to Eq. (11), the UAV motion trajectory will converge to the desired circular orbit with the heading angle command, thus demonstration that the initial heading is consistent with the direction of the guidance vector field. However, the initial heading is generally inconsistent with the guidance vector field, the following section will provide a way for the UAV to converge on the desired heading and prove it.

III. TRACKING CONTROLLER DESIGN

Based on the second chapter of windy and stationary targets, the proposed the Lyapunov guidance vector field method is extended to explain the unknown wind and motion target. Here, we use variable airspeed control and the wind's adaptive estimates to maintain a circular orbit model. In general, the motion target has the same characteristics, which restricts to consider the motion target with a constant forward velocity. However, this method can be applied to the multi-UAV tracking motion target at a constant velocity. We also discuss the limitations of theory and practice and design controller with given kinematic constraints.

A. Variable airspeed controller design

The UAV's dynamic equation is given by Eq. (1). It represents the mathematical model relative to the motion target, the model of adding wind is as follows:

$$\begin{cases} \dot{x} = \mu_1 \cos\psi + W_x - V_{xT} \\ \dot{y} = \mu_1 \sin\psi + W_y - V_{yT} \\ \dot{\psi} = \mu_2 \end{cases} \tag{13}$$

where $\left[W_x, W_y\right]^T$ represents the component of a constant wind velocity in two axes directions, $\left[W_{xT}, W_{yT}\right]^T$ represents the component of the constant inertial target motion velocity in two axes directions. The windy velocity and target motion velocity both affect the dynamics of the model and combine the two effects into one variable, as shown in Eq. (14):

$$\begin{cases} T_x = V_{xT} - W_x \\ T_y = V_{yT} - W_y \end{cases} \tag{14}$$

We treat T_x and T_y as unknown constant, and suppose the availability of the upper bound, hence, T^* satisfies the following formula:

$$\max\left(T_x, T_y\right) \le T^* \tag{15}$$

It encompasses the worst case of the wind and motion target velocities in the coupling effect. Consider the following controller design:

$$\begin{cases} \mu_1 \cos\psi = -\mu_0 \cos\left(\theta - \phi\right) + \hat{T}_x - \upsilon_s \sin\theta \\ \mu_1 \sin\psi = -\mu_0 \sin\left(\theta - \phi\right) + \hat{T}_y + \upsilon_s \cos\theta \end{cases} \tag{16}$$

where $\hat{T}_x$ and $\hat{T}_y$ present adaptive estimates in the case of unknown wind and motion target, υ_s presents a specific signal, and all other symbols have same meaning as before. We define a heading, is given by:

$$\tan\psi = \frac{-\mu_0 \sin\left(\theta - \phi\right) + \hat{T}_y + \upsilon_s \cos\theta}{-\mu_0 \cos\left(\theta - \phi\right) + \hat{T}_x - \upsilon_s \sin\theta} \tag{17}$$

And the airspeed input is as follows:

$$\begin{aligned} \mu_1^2 = &\left[-\mu_0 \sin\left(\theta - \phi\right) + \hat{T}_y + \upsilon_s \cos\theta\right]^2 \\ &+ \left[-\mu_0 \cos\left(\theta - \phi\right) + \hat{T}_x - \upsilon_s \sin\theta\right]^2 \end{aligned} \tag{18}$$

The heading angle is given by Eq. (17), it is different from the obtained heading rate input. Combining Eqs. (13) and (17), we obtain the Eq. (19), as shown in the following formula:

$$\begin{cases} \dot{r} = -\mu_0 \dfrac{r^2 - r_d^2}{r^2 + r_d^2} + \tilde{T}_x \cos\theta + \tilde{T}_y \sin\theta \\ r\dot{\theta} = -\mu_0 \dfrac{2rr_d}{r^2 + r_d^2} - \tilde{T}_x \sin\theta + \tilde{T}_y \cos\theta + \upsilon_s \end{cases} \tag{19}$$

where $\tilde{T}_x = \hat{T}_x - T_x$ and $\tilde{T}_y = \hat{T}_y - T_y$ are adaptive estimation errors. We use the same Lyapunov guidance vector field to define relative motion in the ideal case, as shown in Eq. (20):

$$\begin{cases} \dot{r}_p = -\mu_0 \dfrac{r_p^2 - r_d^2}{r_p^2 + r_d^2} \\ r_p \dot{\theta}_p = -\mu_0 \dfrac{2r_p r_d}{r_p^2 + r_d^2} \end{cases} \tag{20}$$

The defined error signal is given by

$$\begin{cases} e_r = r - r_p \\ e_\theta = \theta - \theta_p \end{cases} \tag{21}$$

and the response error dynamics are given by

$$\begin{cases} \dot{e}_r = -\mu_0 \dfrac{2r_d^2\left(r^2 - r_p^2\right)e_r}{\left(r^2 + r_d^2\right)\left(r^2 + r_p^2\right)} + \tilde{T}_x \cos\theta + \tilde{T}_y \sin\theta \\ \dot{e}_\theta = -\mu_0 \dfrac{2r_d^2\left(r^2 + r_p^2\right)e_r}{\left(r^2 + r_d^2\right)\left(r^2 + r_p^2\right)} + \dfrac{1}{r}\left(-\tilde{T}_x \sin\theta + \tilde{T}_y \cos\theta + \upsilon_s\right) \end{cases} \tag{22}$$

The actual trajectory and guidance filed trajectory have same curve, which shows $r_p\left(0\right) = r\left(0\right)$ and $\theta_p\left(0\right) = \theta\left(0\right)$. Therefore, when the heading angle converges to the angle corresponding to the Lyapunov guidance vector field, the error signal is zero at the initial time.

It is important to obtain the desired heading angle before the adaptive process is initialized. In fact, the built model offers some flexibilities and facilitates in subsequent analysis, while the adaptive estimates $\hat{T}_x$ and $\hat{T}_y$ are also initialized. The

desired heading angle requires not be fully known, but we can be close to the exactly heading angle by using pattern recognition. When the target does not enter the initial loiter circle, we have obtained the exactly heading angle.

For some initial conditions and target motion trajectory, the heading angle of UAV does not convergence to the desired heading angle within a loiter circle. Suppose that the desired heading angle of the motion target is obtained before entering the initial set circle, which will be achieved. However, the target will eventually exit the circular trajectory because the target moves at a constant velocity. Hence, the desired heading angle will be achieved, but it may need more oscillations to converge to the desired circle. For simplicity, we believe that there is enough initial separation time so that the desired heading angle can achieve the purpose of separation within the scope of the initial loiter circle orbit. Thus, the required time of motion target in a circular orbit will be applied to the variable velocity control scheme design.

B. Stability analysis

Before analyzing stability, a parametric projection relationship was introduced to ensure that the motion target estimates evolve within the scope of given T^*.

We define new variables, as shown in Eq. (23):

$$\begin{cases} \hat{T}_x = T^* \tanh \hat{\phi}_x \\ \hat{T}_y = T^* \tanh \hat{\phi}_y \end{cases} \tag{23}$$

where $\hat{\phi}_x$ and $\hat{\phi}_y$ present the unconstrained estimates, the actual parameter value of response is as follows:

$$\begin{cases} T_x = T^* \tanh \phi_x^* \\ T_y = T^* \tanh \phi_y^* \end{cases} \tag{24}$$

Consider the Lyapunov function, as shown in Eq. (25):

$$\begin{aligned} V = {} & \frac{1}{2} e_r^2 + (\mu/2) e_\theta^2 + \left(T^*/\gamma\right)\left(\log\cosh \hat{\phi}_x - \hat{\phi}_x \tanh \phi_x^*\right) \\ & + \left(T^*/\gamma\right)\left(\log\cosh \hat{\phi}_y - \hat{\phi}_y \tanh \phi_y^*\right) + c^* \end{aligned} \tag{25}$$

where c^* represents to be determined constant value. For any $\mu > 0$ and $\gamma > 0$, the function $V(t)$ is positive definiteness. According to the defined motion trajectory in Eq. (22), we calculate the derivative of function $V(t)$, and define the adaptive update algorithm, as shown in the following formula:

$$\begin{cases} \dot{\theta}_x = -\gamma \left[e_r \cos\theta - \mu \dfrac{e_\theta \sin\theta}{r} \right] \\ \dot{\theta}_y = -\gamma \left[e_r \sin\theta + \mu \dfrac{e_\theta \cos\theta}{r} \right] \\ \upsilon_s = -\dfrac{k_\theta \mu_0}{\gamma} \tanh e_\theta + \beta \end{cases} \tag{26}$$

For signal β and the positive constant k_θ, we obtain

$$\begin{aligned} \dot{V} = {} & -\mu_0 \mu \mu_0 \frac{2 r_d^2 \left(r^2 - r_p^2\right) e_r^2}{\left(r^2 + r_d^2\right)\left(r^2 + r_p^2\right)} - \frac{k_\theta}{r} e_\theta \tanh e_\theta \\ & - \mu \mu_0 \frac{2 r_d \left(r + r_p\right) e_r e_\theta}{\left(r^2 + r_d^2\right)\left(r^2 + r_p^2\right)} + \frac{\mu \beta e_\theta}{r} \end{aligned} \tag{27}$$

where the parameter γ represents the rate of an adaptive learning, in other words, which can control how to rapid adapt to the Eq. (26). To eliminate the uncertainty of the signal in Eq. (28), we define β, as follows in the Eq. (28):

$$\beta = \frac{2 \mu_0 r_d \left(r + r_p\right) r e_r}{\left(r^2 + r_d^2\right)\left(r^2 + r_p^2\right)} \tag{28}$$

and we obtain:

$$\dot{V} = -\mu_0 \frac{2 r_d^2 \left(r^2 - r_d^2\right) e_r^2}{\left(r^2 + r_d^2\right)\left(r^2 + r_p^2\right)} - \frac{k_\theta \mu_0}{\gamma r} e_\theta \tanh e_\theta \le 0 \tag{29}$$

From Eqs. (19) and (23), we obtain easily the Lyapunov function is less than zero if $\gamma > 0$. The constant c^* is still to be determined in Eq. (25). Since the initial values of errors e_r and e_θ are zero, when it is assumed that the initial value of the adaptive estimation $\hat{\phi}_x$ and $\hat{\phi}_y$ are also zero and whenever $\hat{\phi}_x = \phi_x^*$ and $\hat{\phi}_y = \phi_y^*$, which the third and fourth orders of the function have a minimum value. To prove the positive definiteness of the Lyapunov function, we define c^*, as shown in the following formula:

$$c^* = \left(T^*/\gamma\right) \begin{bmatrix} \left|\log\cosh \phi_x^* - \phi_x^* \tanh \phi_x^*\right| \\ + \left|\log\cosh \phi_y^* - \phi_y^* \tanh \phi_y^*\right| \end{bmatrix} \tag{30}$$

where c^* is inversely proportional to γ, and $1/2 e_r^2 \le V(t) \le V(0) = c^*$, here $\left|e_r(t)\right| \le \sqrt{2c^*}$.

According to the above formulas, we establish the upper bound of c^*, as shown in the following formula:

$$c^* \le \frac{2 \log 2T^*}{\gamma} \tag{31}$$

Therefore, the maximum radius error of the trajectory of the motion target is reduced by increasing the learning rate parameter γ.

We can obtain bound of derivative V, combining the $\mu_{12} \ge \mu_0 - \Delta V_{\max}$ and $r_d \le r_i(t) \le r_{i0}$, as shown in the following formula:

$$\begin{aligned} \dot{V} \le {} & -\Delta V_{\max} \frac{r_d}{R_i^2} \Big[\left(\left|\tanh \delta\theta_1\right| - \left|\tanh \delta\theta_2\right|\right)^2 + \left(\left|\tanh \delta\theta_2\right| - \left|\tanh \delta\theta_3\right|\right)^2 \\ & + \cdots + \left(\left|\tanh \delta\theta_{n-1}\right| - \left|\tanh \delta\theta_n\right|\right)^2 + \left(\left|\tanh \delta\theta_n\right| - \left|\tanh \delta\theta_1\right|\right)^2 \Big] \\ & + \sum_{i=1}^{n} \left[\frac{2\mu_0}{r_d} - \lambda r_d \left(\mu_0 - \Delta V_{\max}\right) \right] \frac{r_i^2 - r_d^2}{r_i^2 + r_d^2} \end{aligned} \tag{32}$$

Choosing:

$$\lambda > \frac{2\mu_0}{r_d^2 \left(\mu_0 - \Delta V_{\max}\right)} \tag{33}$$

when $\dot{V} \le 0$, it implies: $\lim_{t \to \infty} \left|\tanh \delta\theta_i\right| = \bar{T} \quad \forall\, i$ (34)

where $\bar{\theta}$ and $\bar{T}$ are the finite constant. For any i, we obtain $\delta\theta_i = \bar{\theta}$ when $t \to \infty$.

Now we define the angular error, as shown in the following formula:

$$\begin{cases} e_{12} = \theta_1 - \theta_2 \\ e_{23} = \theta_2 - \theta_3 \\ \quad \vdots \\ e_{n-1,n} = \theta_{n-1} - \theta_n \\ e_{n1} = \theta_n - \theta_1 \end{cases} \tag{35}$$

and when $t \to \infty$, we can obtain the relationship of between the angular spacing and the angular error from Eq. (35), as follows

$$\begin{bmatrix} \delta\theta_1 \\ \delta\theta_2 \\ \delta\theta_3 \\ \vdots \\ \delta\theta_{n-1} \\ \delta\theta_n \end{bmatrix} = \begin{bmatrix} \bar{\theta} \\ \bar{\theta} \\ \bar{\theta} \\ \vdots \\ \bar{\theta} \\ \bar{\theta} \end{bmatrix} = \begin{bmatrix} \frac{1}{2} & 0 & 0 & \cdots & 0 & -\frac{1}{2} \\ -\frac{1}{2} & \frac{1}{2} & 0 & 0 & \cdots & 0 \\ 0 & -\frac{1}{2} & \frac{1}{2} & 0 & \cdots & 0 \\ \vdots & \cdots & \ddots & \ddots & 0 & 0 \\ 0 & \cdots & 0 & -\frac{1}{2} & \frac{1}{2} & 0 \\ 0 & 0 & \cdots & 0 & -\frac{1}{2} & \frac{1}{2} \end{bmatrix} \begin{bmatrix} e_{12} \\ e_{23} \\ e_{34} \\ \vdots \\ e_{n-1,n} \\ e_{n1} \end{bmatrix} + \begin{bmatrix} \pi \\ 0 \\ 0 \\ \vdots \\ 0 \\ -\pi \end{bmatrix} \tag{36}$$

Further, the sum of the all angular differences is zero, as follows:

$$e_{12} + e_{23} + e_{34} + \cdots + e_{n-1,n} + e_{n1} = 0 \tag{37}$$

From Eq.(37),we can see that there are $n+1$ equations to be determined. Solving the $n+1$ equations, we obtain $\bar{\theta} = 0$, $e_{ij} = (2\pi/n)\ \forall\ i, j$ and the equivalent angular spacing. ($t \to \infty$)

IV. SIMULATION RESULTS

Aiming at the problem of the multi-UAV cooperative tracking, we design a control laws and demonstrate the validity of the designed control laws. The simulation experiments are carried out for only the minimal persistent information architecture. The nonminimally persistent information architecture have same properties, so the analysis process does not include the associated results. In the process of the simulation, we study the tracking characteristics of four UAVs in stationary targets and two UAVs around motion targets.

The setup initial condition: $\mu_0 = 20\text{m}/s$, $r_d = 300m$, $\Delta V_{\max} = 5m/s$, $x_{10} = 500m$, $y_{10} = 500m$, $\psi_{10} = 0$, $x_{20} = -800m$, $y_{20} = -600m$, $\psi_{20} = \pi/2$, $x_{30} = -500m$, $y_{30} = 500m$, $\psi_{30} = \pi$, $x_{40} = 700m$, $y_{40} = -100m$, $\psi_{10} = -\pi/4$. We show the simulation results, as shown in Figs. 1 to 4:

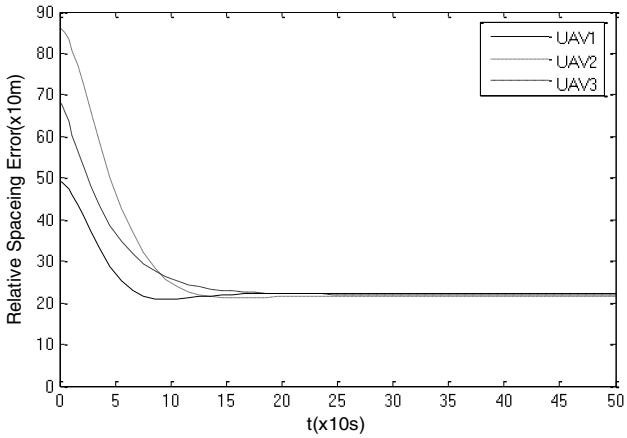

Fig.1 The relative distance of between UAV and stationary target

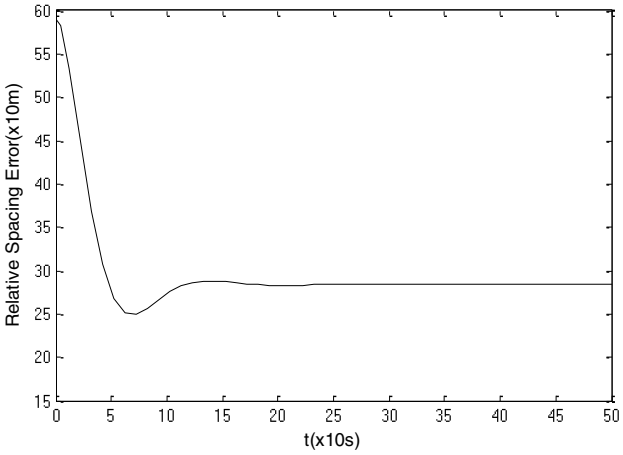

Fig.2 The relative distance error between two UAV around the stationary

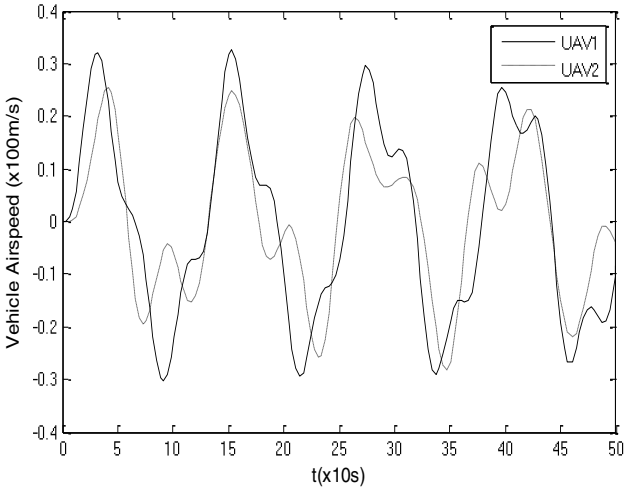

Fig.3 The airspeed command of between the spacing and maintaining circular orbit around

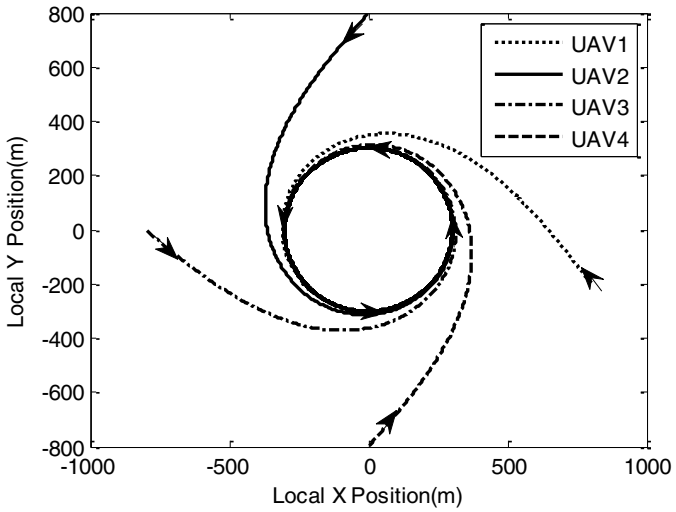

Fig. 4 The four-UAV motion trajectories around the stationary target

The Fig. 1 adopts the three UAVs formation as a control object and presents the relative distance error between the UAV and the target in the process of tracking motion target, which shows a trend of tending to level state after rapid decline. As can be seen from the figure 4, the UAV formation consists of one leader and two followers and is rapidly close to the target. From 1s to 15s, the leader of formation is in front of the follower, and the forward velocity is larger than two followers. In addition, the UAV tracks target with the fastest velocity and most optimized path before the UAV is close to the target; when the UAV is very close to the target, the UAV formation can achieve the purpose of cooperative tracking with a fixed geometric shape.

The Figs. 2 and 3 adopt the two UAVs as a control object. As can be seen from the figure 3, it shows that the relative distance error between two UAVs around the stationary target, and presents a tendency to decrease and then increase. In the process of the tracking the target with the shortest time, the multi-UAV will be affected by air resistance because the wingtip will generate the vortex effect. From figure 4, it presents that the airspeed command of between the spacing and maintaining circular orbit around the motion target, and shows a trend of the cooperative formation flight, but there is a certain delaying phenomenon. In the process of the cooperative tracking controller, each UAV is equipped with a control command sensor. Especially, there is a phenomenon that the received information is deviated in the process of high-speed flight.

Fig. 4 shows the four UAVs' trajectories around the stationary target. Initially, the UAV has multiple headings and loiter circles, all of which converge to the desired heading along the Lyapunov guidance vector field. When all UAVs reach a loiter circular orbit with the prescribed distance, the variable airspeed controllers can achieve the desired angular spacing.

V. CONCLUSION

In this paper, we design the control laws and prove the stability of tracking motion target based on the Lyapunov guidance field, which is only theoretical research. For the path planning of a single UAV, we present a proof of heading convergence to address the previously neglected timescale issue, and then propose a novel heading convergence method. We also analyze the guidance vector field by using the analytical solution method, which provides an advantage for the combination of theory and practice. In the case of unknown wind and motion target, we use the adaptive estimates to ensure the stability of the circular trajectory. For multi-UAV formation, the variable airspeed controller can achieve the desired spatial position. At present, the designed cooperative tracking controller is not embedded into the real UAV due to the limitation of conditions, the next major focus of our research will be to implement the designed controller in a practical application.

REFERENCES

[1] Oh K K, Park M C, Ahn H S. A survey of multi-agent formation control. Pergamon Press, Inc. 2015.

[2] Lin Z, Broucke M, Francis B. Local control strategies for groups of mobile autonomous agents. Automatic Control IEEE Transactions on, 2004, 49(4):622-629.

[3] Dimarogonas D V, Kyriakopoulos K J. A connection between formation infeasibility and velocity alignment in kinematic multi-agent systems. Automatica, 2008, 44(10):2648-2654.

[4] Ren W, Atkins E. Distributed multi-vehicle coordinated control via local information exchange. International Journal of Robust & Nonlinear Control, 2010, 17(10-11):1002-1033.

[5] Lin Z, Francis B, Maggiore M. Necessary and sufficient graphical conditions for formation control of unicycles. IEEE Transactions on Automatic Control, 2005, 50(1):121-127.

[6] Krick L, Broucke M E, Francis B A. Stabilization of infinitesimally rigid formations of multi-robot networks. Decision and Control, 2008. Cdc 2008. IEEE Conference on. IEEE, 2009:477-482.

[7] Oh K K, Ahn H S. Formation control of mobile agents based on inter-agent distance dynamics. Automatica, 2011, 47(10):2306-2312.

[8] Dorfler F, Francis B. Geometric Analysis of the Formation Problem for Autonomous Robots. IEEE Transactions on Automatic Control, 2010, 55(10):2379-2384.

[9] Cao M, Morse A S, Yu C, et al. Maintaining a Directed, Triangular Formation of Mobile Autonomous Agents. Communications in Information & Systems, 2010, 11(11):1-16.

[10] Oh K, Ahn H. Distance-based undirected formations of single-integrator and double-integrator modeled agents in n-dimensional space. International Journal of Robust & Nonlinear Control, 2014, 24(12):1809-1820.

[11] Nie Z, Zhang X, Guan X. UAV formation flight based on artificial potential force in 3D environment. Chinese Control and Decision Conference. 2017:5465-5470.

[12] Cetin O, Yilmaz G. Real-time Autonomous UAV Formation Flight with Collision and Obstacle Avoidance in Unknown Environment. Journal of Intelligent & Robotic Systems, 2016, 84(1-4):1-19.

[13] Bullo F. Optimal sensor placement and motion coordination for target tracking. Pergamon Press, Inc. 2006.

[14] Abu-Jbara K, Alheadary W, Sundaramorthi G, et al. A robust vision-based runway detection and tracking algorithm for automatic UAV landing. International Conference on Unmanned Aircraft Systems. IEEE, 2015:1148-1157.

[15] Kingston D, Beard R. UAV Splay State Configuration for Moving Targets in Wind. Advances in Cooperative Control and Optimization. Springer Berlin Heidelberg, 2007:109-128.

[16] Marshall J A, Broucke M E, Francis B A. Pursuit formations of unicycles. Pergamon Press, Inc. 2006.

[17] Savla K, Bullo F, Frazzoli E. On Traveling Salesperson Problems for Dubins ' vehicle: stochastic and dynamic environments. Decision and Control, 2005 and 2005 European Control Conference. Cdc-Ecc '05. IEEE Conference on. IEEE, 2005:4530-4535.

View publication stats